

Biogenic Synthesis and Characterization of Silver Nanoparticles: Evaluation of Their Larvicidal, Antibacterial, and Cytotoxic Activities

Shanmugam Mahalingam,¹ Praveen Kumar Govindaraji,¹ Vasthi Gnanarani Solomon, Hema Kesavan, Yalini Devi Neelan, Senthil Bakthavatchalam,* Junghwan Kim,* and Prakash Bakthavatchalam



Cite This: *ACS Omega* 2023, 8, 11923–11930



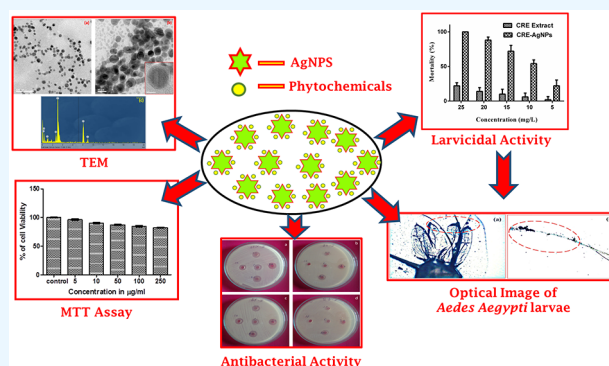
Read Online

ACCESS |

Metrics & More

Article Recommendations

ABSTRACT: To explore the larvicidal activity of the silver nanoparticles (AgNPs) synthesized using the ethanolic *Catharanthus roseus* flower extract (CRE) against the larvae of *Aedes aegypti* (*A. aegypti*), AgNPs were synthesized by an eco-friendly method and characterized by Ultraviolet–Visible (UV–Vis) spectroscopy, Fourier Transform Infrared spectroscopy (FTIR), X-Ray Diffraction (XRD), Particle Size Analysis, Transmission Electron Microscopy (TEM), and Energy-Dispersive X-Ray spectrometry (EDX) analysis. The resultant AgNPs showed a spherically well-defined, highly stable, and monodispersed shape with an average particle size ranging from 15 to 25 nm. The absorbance of the AgNPs was measured by using a UV–Vis spectrophotometer at a wavelength of 416 nm. The presence and binding of the phenolic functional group with the AgNPs were confirmed using FTIR analysis. Particle size analysis revealed an average particle diameter of 90 nm with 80 % distribution. XRD analysis revealed the highly crystalline nature of the CRE-AgNPs. The LC₅₀ and LC₉₀ values of CRE-AgNPs and the extract were calculated. The mortality percentage of the extract and synthesized CRE-AgNPs was observed after 24 h. The maximum larvicidal activity with 100 % mortality of *A. aegypti* was observed in AgNPs synthesized using ethanolic CRE. The LC₅₀ and LC₉₀ values are 8.963 and 20.515 ppm for CRE-AgNPs against *A. aegypti* larvae, respectively. The CRE-AgNPs revealed superior antibacterial activity against human pathogenic bacteria; the zone of inhibition (ZOI) was measured for all of the pathogens, and the results revealed that different concentrations of CRE-AgNPs showed a remarkable ZOI of about (a) 10–14 mm for *Salmonella typhimurium*, (b) 6–11 mm for *Bacillus subtilis*, (c) 11–14 mm for *Enterococcus faecalis*, and (d) 9–10 mm for *Shigella boydii*. The maximum ZOI was observed in *E. faecalis*. Impeccably, the cytotoxicity of CRE-AgNPs at 250 $\mu\text{g}/\text{mL}$ is 82% against the HaCaT cell lines. The synthesized CRE-AgNPs showed maximum effectiveness of paradoxical activity on mosquito larvae.



1. INTRODUCTION

Mosquitoes are mainly responsible for the spread/or transmission of lethal diseases, which include malaria, Japanese encephalitis, lymphatic filariasis, yellow fever, dengue, and chikungunya. Dengue and chikungunya are epidemics in the tropical and subtropical regions; 390 million people are infected worldwide, and over 96 million are said to show a clinical manifestation.^{1,2} Worldwide, healthcare professionals and health officials are mainly concentrating on dengue fever, which has become a key public health risk. Although the vaccine is being developed, there is still no proper treatment for dengue fever. Currently, about 40% of the world's population is at risk of dengue infection.^{3,4} Global transmission of dengue (DENV) and chikungunya (CHIKV) viruses has increased in recent years, and all four serotypes of dengue virus are rapidly transmitted by *Aedes aegypti* in Asia, Africa, and America. These mosquitoes are responsible for the trans-

mission of yellow fever and DENV and also act as a main carrier for Zika virus fever. DENV and CHIKV belong to the arboviruses; they are arthropod-borne viruses having a single-stranded RNA genome. DENV belongs to the *Flaviviridae* family, and CHIKV belongs to the *Togaviridae* family.⁵ Mosquito larvae are usually targeted through insect growth regulators, insecticide-treated bed nets, organophosphates, and indoor residual spraying, which are mainly responsible for reducing transmission in tropical countries. Increased use of the abovementioned chemicals during outbreak has negative

Received: November 24, 2022

Accepted: March 13, 2023

Published: March 23, 2023



effects on the environment and human health. Vector control is said to be a serious problem in developing countries like India due to the lack of socioeconomic status and general awareness. Therefore, it is essential to find an alternative insecticide that is low-cost, eco-friendly, and effective. To face the abovementioned challenge, researchers are working on potential and innovative environmental control tools.^{2,6}

Nanoparticles have attracted the attention of researchers due to their comprehensive applications and for the enhancement in the field of materials science, catalysts at the nanoscale, and electronics. Generally, nanoparticles are considered to exhibit new or improved physicochemical and biological properties as compared to bulk materials based on specific characteristics such as size, shape, and charge distribution. In the current scenario, worldwide scientists have focused on cost-effective nanomaterials and their use as an antimicrobial agent to eradicate infectious diseases. Biogenic synthesis of nanoparticles and their application was increased due to their properties, cost-effectiveness, and low virulence. These greener nanomaterials have an enormous role in diagnosis, sensing, and other biomedical applications. The greater advantage of biosynthesized nanoparticles is that there is no necessity for any physical factors like high energy, temperature, and pressure during the biogenic synthesis process. The plant extract is generally used for the synthesis of silver, platinum, gold, copper, and titanium nanoparticles, which have potential antioxidant, anticancer, and antimicrobial properties.^{7–9} Interestingly, silver was used as a therapeutic agent, and there is an urge in utilizing greener nanoparticles for anticancer, antimicrobial, and antilarvicidal activities in recent times.^{10–12} AgNPs are widely used in the field of medicine, agricultural science, and biotechnology due to the advantage of low cost, less toxicity, surface plasmons, and their physicochemical properties. Medicinal plants generally have biosurfactant molecules such as alkaloids, saponins, tannins, glycosides, flavonoids, and phenols. Thus, the materials prepared by the green synthesis method are a potential candidate for larvicidal activity and reducing the accumulation of toxic residues in the aquatic organisms.^{13,14}

According to the World Health Organization (WHO), most developing countries mainly depend on traditional plant-based medicines for healthcare necessities. A rich source of biologically active compounds is presented in the Apocynaceae family. *Catharanthus roseus* is one of the most important medicinal plants from the Apocynaceae family. The flower of this plant is used in India by Ayurvedic physicians for the treatment of dermatitis, eczema, acne, and skin problems. It is very interesting that around 130 minor constituents of alkaloids are produced by this plant.¹⁵ In addition, the phytochemicals like alkaloids, terpenoids, and polyphenolic content were used in the treatment of diabetes, blood pressure, cancer, and asthma.¹⁶

Using plants and herbs for the synthesis of AgNPs is found to be low-cost, eco-friendly, safer, and also less toxic to humans and other organisms that depend on aquatic environments. The current study deals with the larvicidal activity of the AgNPs synthesized using ethanolic *C. roseus* flower extract (CRE) to control the growth of the *A. aegypti* larvae.

2. MATERIALS AND METHODS

2.1. Chemicals. Silver nitrate (AgNO₃, 99.9 % purity) and ethanol were procured from Sigma-Aldrich, India.

2.2. Preparation of Ethanolic *C. roseus* Flower Extract.

Fresh *C. roseus* flowers were obtained from the local market for the synthesis of AgNPs. The flowers were authenticated by taxonomists. Flowers were washed three times with distilled H₂O and then dried in the shade. The flowers were mechanically crushed using agate mortar into fine powder. The powdered flowers (2 g) were suspended in 100 mL of C₂H₅OH after optimization.¹⁷ After a few hours, ethanol was filtered, and the ethanolic *C. roseus* flower extract was kept at 5 °C for further use.

2.3. Preparation of Silver Nanoparticles. Silver nitrate solution (1 mmol, 100 mL) was taken in a 250 mL conical flask; 5 mL of ethanolic CRE was added to the AgNO₃ solution, and the mixture was sonicated for 30 min (ultrasonic power of 100 W and frequency of 30 kHz). After sonication, the color changed from yellow to dark brown, which indicated the formation of AgNPs (Figure 1). These particles were referred to as CRE-AgNPs (*C. roseus* extract silver nanoparticles). This reaction was kept in the dark condition at room temperature or 37 °C. Then, the impurities were removed by centrifuging the solution at 10,000 rpm for 30 min at 4 °C. The reaction was observed at regular intervals (0, 10, 20, 30, and 40 min) using a UV–Vis spectrophotometer for monitoring the AgNP formation.

2.4. Characterization of Silver Nanoparticles. The absorption spectra ranging from the wavelength of 300 to 700 nm were measured using a T90 UV–Vis spectrophotometer (PG Instruments Ltd.). The FTIR spectrum was recorded by using a Bruker FTIR spectrometer with a wavelength ranging from 400 to 4000 cm⁻¹ at a resolution of 4 cm⁻¹. The X-Ray diffraction (XRD) studies were carried out using a powder X-ray diffractometer, Rigaku Mini flux II, using the Cu K α radiation with a wavelength (λ) of 1.5406 Å. The particle size of the CRE-AgNPs were analyzed using a Malvern Zetasizer Nano series. For Transmission Electron Microscopy (TEM) studies, a few drops of CRE-AgNPs were dripped on a copper grid and images were obtained using high-resolution transmission electron microscopy (HRTEM, FEI Tecnai TM G2 F20) with an operating voltage of 120 kV. Energy-dispersive X-ray spectroscopy (EDX) was used to analyze the chemical composition. The optical image of mosquito larvae was captured using an Optical Microscope Nikon ECLIPSE LV100N POL.

2.5. Insect Rearing. The *A. aegypti* larvae were collected from stagnant water in Chennai, which was identified at Kings Institute of Preventive Medicines, Guindy, Chennai, India. Early fourth-instar larvae of *A. aegypti* were locally collected and kept in plastic enamel trays containing dechlorinated tap water. They were maintained as previously reported by Patil et al.^{18,19}

2.6. Larvicidal Bioassay. The larvicidal activities were assessed by the WHO procedure (1996) with some modifications, as per the method of Rahuman et al.^{20,21} The CRE (1 mL) was first dissolved in 100 mL of distilled water (stock solution). From the stock solution, a 100 ppm solution was prepared with dechlorinated tap water for the bioassay test of the CRE.

For the bioassay test, five batches of 20 larvae in 249 mL of dechlorinated water and 1 mL of desired extract concentration were added in a beaker. The control was set up with dechlorinated tap water. The dead larvae numbers were counted after 24 h of exposure, and the mortality percentage was reported from the average of five replicates. In

experimental media, the larval mortality was found to be 100%, and it was selected for the dose–response bioassay.

The toxicity test of the CRE-AgNPs was performed by placing 20 mosquito larvae in 200 mL of double-distilled H₂O. The CRE-AgNPs (100 mg) were dissolved in 1 L of Milli-Q water (stock solution). In this study, from the stock solution, different concentrations were varied from 25, 20, 15, and 10 to 5 ppm. Each test included a set of the control group (distilled water) with five replicates of each individual concentration. Mortality was assessed after 24 h to determine the acute toxicities on fourth-instar larvae of *A.aegypti*.

2.7. Dose–Response Bioassay. Based on the preliminary screening results, crude CRE and CRE-AgNPs were subjected to a dose–response bioassay against the larvae of *A. aegypti*. Different concentrations ranging from 25, 20, 15, and 10 to 5 ppm (CRE and CRE-AgNPs) were prepared for larvicidal activity. The number of dead larvae was counted after 24 h of exposure, and the percentage of mortality was reported from the average of five replicates.

2.8. Antimicrobial Activity. The antimicrobial activities of green-synthesized CRE-AgNPs were studied by the well diffusion method against pathogenic organisms like (a) *Salmonella typhimurium* (ATCC 14028), (b) *Bacillus subtilis* (ATCC 6051), (c) *Enterococcus faecalis* (ATCC 29212), and (d) *Shigella boydii* (ATCC 12027). The pure cultures were subcultured on a Muller–Hinton broth at 35 °C on a rotary shaker at 250 rpm. Each strain was swabbed uniformly on the individual petri plates using a sterile cotton swab. The wells (5 nos.) were made on Muller–Hinton agar of diameter (6 mm) by using gel puncture. 1 μL of Streptomycin was used as a control, which was placed in a well on each plate. About 10, 20, 30, and 40 μL of CRE-AgNP solution were dripped into the remaining wells. Streptomycin was used as a control. These plates were incubated at 35 °C for 24 h.²²²³ After incubation, the obtained zones of inhibition (ZOI) were measured.

2.9. MTT Assay. The cytotoxicity of HaCaT cell lines against CRE-AgNPs was measured by the MTT (3-(4, 5-dimethylthiazol-2-yl)-2, 5-diphenyl tetrazolium bromide) assay.²⁴ The HaCaT cells were plated separately in 96-well plates at a concentration of 10⁵ cells/well. After 24 h, the cells were washed twice with 100 μL of serum-free medium and starved for an hour at 37 °C. After starvation, the cells were treated with different concentrations of CRE-AgNPs (10–500 μg/mL) for 24 h. At the end of the treatment period, the medium was aspirated and serum-free medium containing MTT (0.5 mg/mL) was added and incubated for 4 h at 37 °C in a CO₂ incubator.

The MTT-containing medium was then discarded, and the cells were washed with PBS (200 μL). Then, the crystals were dissolved in 100 μL of DMSO, and this was properly mixed. The spectrochemical absorbance of the purple-blue formazan dye was measured at 570 nm by using a microplate reader (Bio-Rad 680). The cytotoxicity results were plotted by using Graph pad prism (version 6.0) software.

2.10. Statistical Analysis. The average larvae mortality rate was subjected to probit analysis to calculate LC₅₀ and LC₉₀ values by utilizing SPSS (version 16.0) software. The values were expressed in terms of (SD ± n = 5) replicates.

3. RESULTS AND DISCUSSION

Silver nanoparticles were synthesized using the ethanolic *C. roseus* flower extract. Interestingly, formations of CRE-AgNPs were observed within 30 min of sonication. The pure, colorless

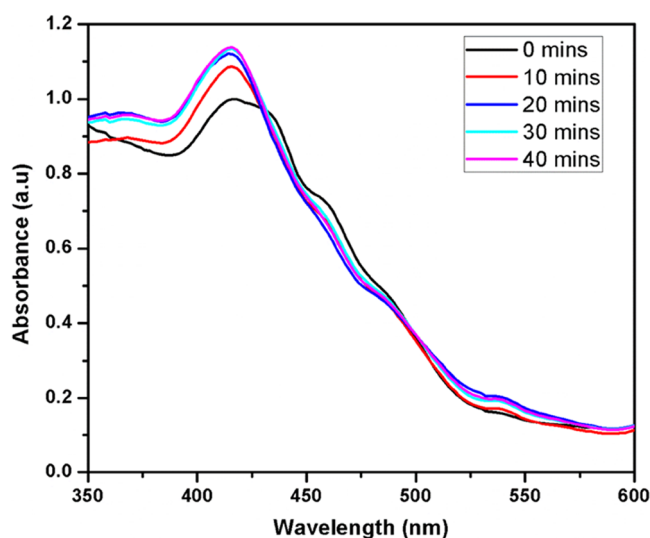


Figure 1. UV–vis spectrum of CRE-AgNPs at different time periods (0 to 40 min).

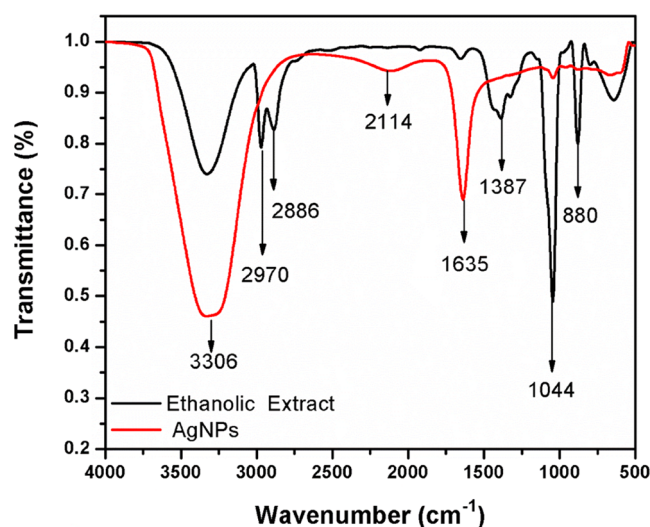


Figure 2. FTIR spectra of CRE and CRE-AgNPs.

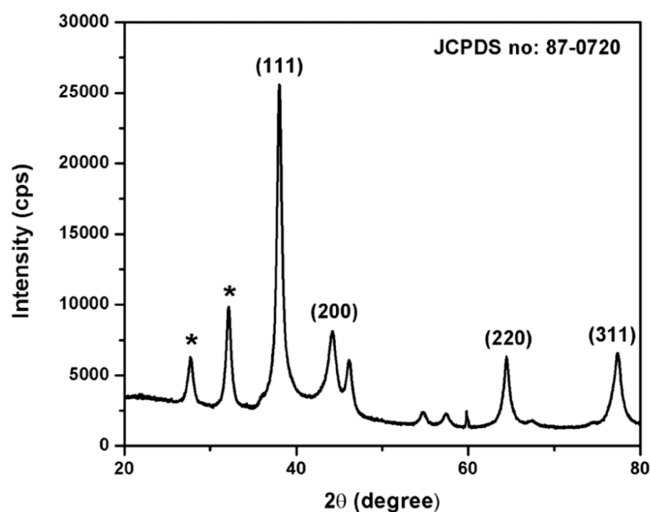


Figure 3. XRD patterns of CRE-AgNPs.

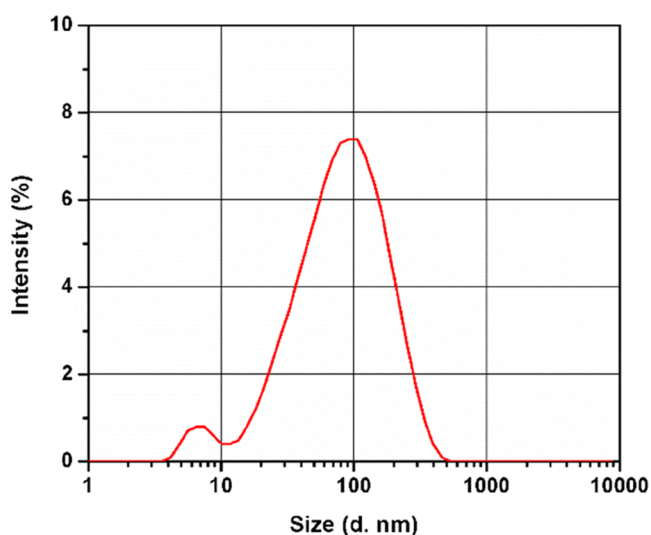


Figure 4. Particle size distribution of CRE-AgNPs.

AgNO_3 solution was added to the extract. The dark brown color changes were observed due to the reduction of AgNO_3 salt to AgNPs and the excitation of surface plasmon resonance (SPR).^{25,26} The UV-Vis results show that the SPR band was observed at 416 nm, without any shift in the wavelength, as shown in Figure 1.

The FTIR analysis was carried out to identify the possible interaction of CRE-AgNPs with the functional groups present in the CRE. The FTIR analysis of the CRE and CRE-AgNPs is

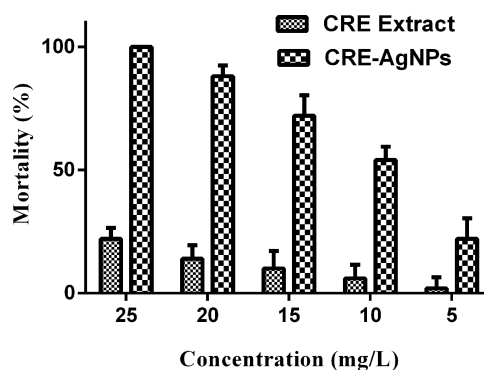


Figure 6. Graph showing the mortality (%) rate of larvae after exposure at different concentrations of CRE and CRE-AgNPs.

Table 1. Larvicidal Activity of CRE-AgNPs against *A. aegypti* Larvae^a

concentration (ppm)	mortality (%)	LC ₅₀ (ppm)	LC ₉₀ (ppm)
25	100.000 ± 0.00	8.963	20.515
20	88.000 ± 4.47		
15	72.000 ± 8.36		
10	54.000 ± 5.48		
5	22.000 ± 8.36		

^aControl: Nil; Values are represented as Mean ± S.D; $n = 5$.

shown in Figure 2. The FTIR spectrum of CRE shows five major peaks at 3306, 2970, 2886, 1387, 1044, and 880 cm^{-1} . The peak at 3306 cm^{-1} was due to the stretching vibration of

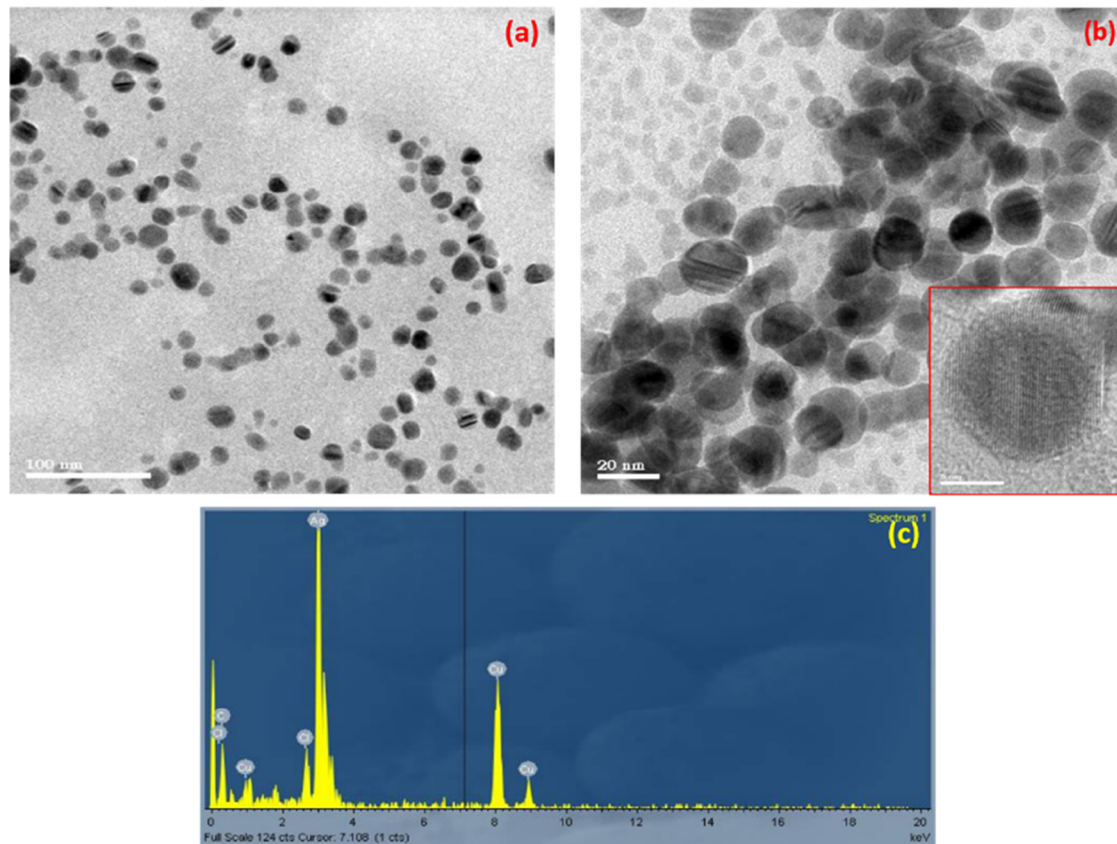


Figure 5. HRTEM images of spherically shaped CRE-AgNPs at different scale bars of (a) 100 nm, (b) 20 nm, and 5 nm for the inset show the lattice arrangement. (d) Energy-dispersive X-ray spectrum shows the elemental presence of silver.

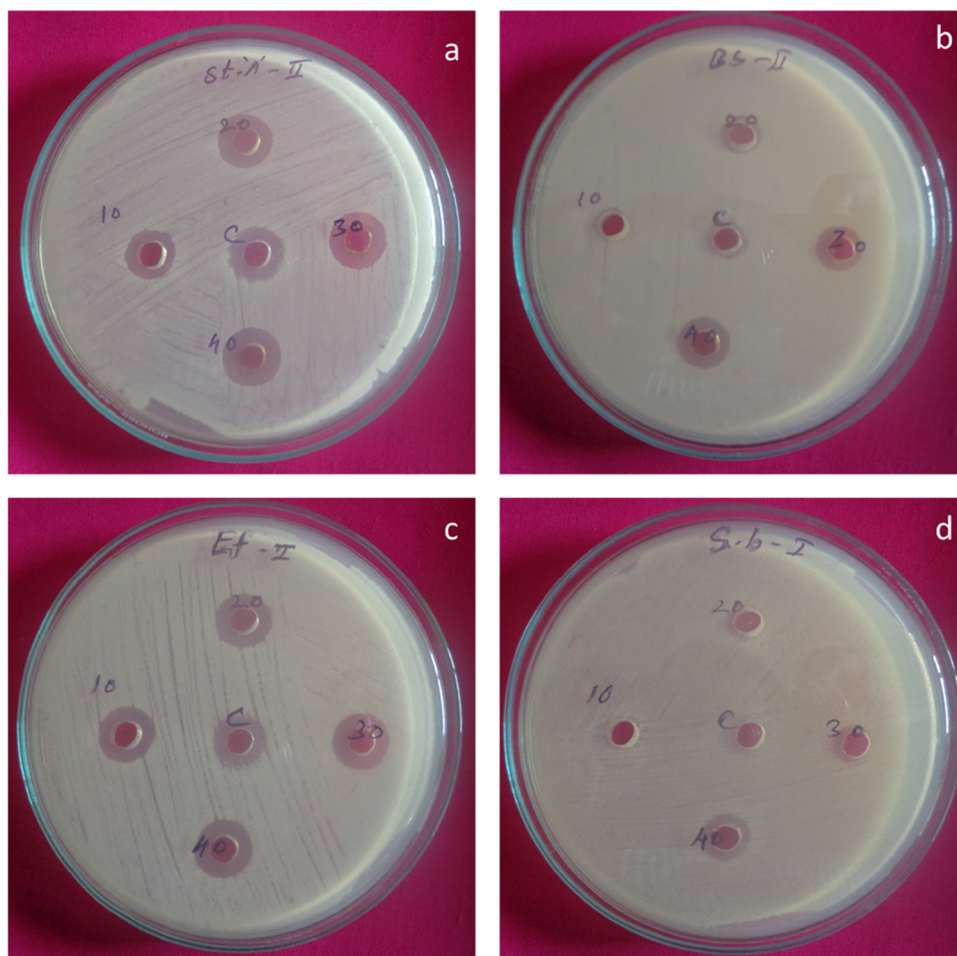


Figure 7. Antibacterial potential of CRE-AgNPs against (a) *S. typhimurium*, (b) *B. subtilis*, (c) *E. faecalis*, and (d) *S. boydii* by the well diffusion assay.

Table 2. Zone of Inhibition of CRE-AgNPs against (a) *S. typhimurium*, (b) *B. subtilis*, (c) *E. faecalis*, and (d) *S. boydii*

concentrations (μL)	zone of inhibition (mm)			
	<i>S. typhimurium</i>	<i>B. subtilis</i>	<i>E. faecalis</i>	<i>S. boydii</i>
control (streptomycin)	7	7	11	
10	10	6	12	
20	12	7	13	
30	13	10	13	9
40	14	11	14	10

OH in alcoholic and phenolic functional groups. The bands at 2970 and 2887 cm^{-1} correspond to a strong stretching vibration of CH functional groups. The bands at 1387 and 1044 cm^{-1} correspond to the symmetric stretching of COO^{-1} and C–O stretch of functional groups, respectively. The peak at 880 cm^{-1} is attributed to the out-of-plane CH_2 . The FTIR spectrum of CRE-AgNPs shows three distinct peaks at 3306, 2114, and 1635 cm^{-1} . The peaks at 3306 and 2114 cm^{-1} correspond to the stretching vibration of OH in the alcoholic and phenolic and $\text{C}\equiv\text{C}$ of functional groups, respectively. The peak at 1635 cm^{-1} is due to the stretching vibration of $\text{C}=\text{O}$ functional groups. Hence, FTIR spectral analysis confirms the presence of specific moieties on the CRE-AgNPs, and these moieties correspond to the constituent of *C. roseus* flower, such as polyphenols, terpenoids, and alkaloids, which has been confirmed from the study. Hence, we conclude that these

compounds are responsible for the surface coating and reduction of AgNO_3 .^{27–29}

Figure 3 shows the XRD analysis of CRE-AgNPs, which indicates the high crystallinity nature of the polycrystalline properties of nanoparticles. Four distinct Bragg reflections with the 2θ values of 38.02, 44.16, 64.44, and 77.34° correspond to the lattice planes of 111, 200, 220, and 311, respectively. The obtained data matched well with the face-centered cubic (FCC) symmetry of pure silver (JCPDS file no; 87-0720). The unassigned peaks indicated the presence of bioorganic phase crystals.³⁰ The additional peak obtained at 27 °C might be due to the unreduced AgNO_3 .^{31,32} The average crystalline size is 10 nm, which is calculated by using the Debye Scherrer formula.

The quantitative size distribution of the CRE-AgNPs is determined using dynamic light scattering (DLS). The CRE-AgNPs had an average diameter of 89 nm, which was measured using a Zetasizer, as shown in Figure 4. It also revealed that 80 % of the distribution of CRE-AgNPs is around 90 nm.^{26,31}

Figure 5 shows the TEM images of CRE-AgNPs. TEM reveals that the CRE-AgNPs are spherical in shape with a well-defined structure. The particle size ranges from 15 to 25 nm. It was observed that there was no physical interaction between the particles. The inset image shows the well-defined fringes, which indicate the highly crystalline nature of CRE-AgNPs, which is in good agreement with XRD results.³³ The particles are monodisperse in nature and CRE-AgNPs are stabilized with capping agents, which are presented in the extract (i.e.,

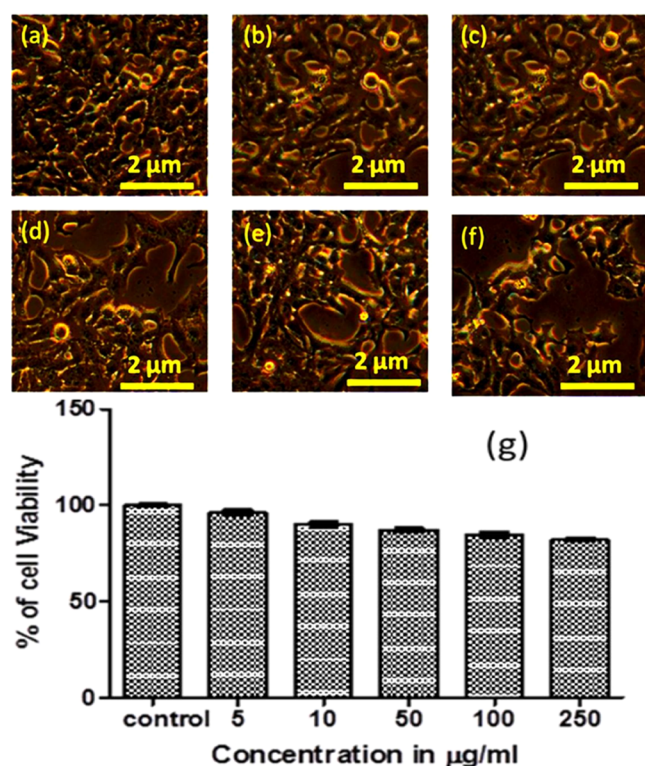


Figure 8. In vitro cytotoxicity effect of CRE-AgNPs in HaCaT cell lines. (a) Control, (b–f) cells treated with 5, 10, 50, 100, and 250 µg/mL and (g) cell viability percentage of CRE-AgNPs.

polyphenol, alkanoid, saponins, etc.) as confirmed by FTIR analysis shown in Figure 5a,b. These capping agents are effective barriers against the agglomeration of CRE-AgNPs, which is the major drawback of the chemically synthesized nanoparticles.^{29–33} The EDX spectrum also confirms the dominant presence of silver with the sharp peak in Figure 5d.³⁴

The mortality percentage of fourth-instar larvae *A. aegypti* exposed to CRE and CRE-AgNPs for 24 h was determined.^{35–37} The mortality percentage was observed for different concentrations (25 to 5 ppm) of CRE and CRE-AgNPs. Distilled H₂O is used as a control. The mortality percentage with respect to different concentrations of CRE and CRE-AgNPs is shown in Figure 6. Mouchet et al.³⁸ showed the highest mortality rate of 85 % against *Xenopus laevis* larvae with a concentration of 500 ppm for double-walled carbon

nanotubes. The maximum larvicidal activity was reported for AgNPs synthesized using *Tinospora*³⁹ and *Nelumbo nucifera*⁴⁰ against the larvae of *Culex quinquefasciatus*. In this study, a maximum mortality of 100 % was observed in 25 ppm CRE-AgNPs. However, the same concentration of pure ethanolic extract shows only 22 % mortality. The mortality percentage of the CRE and CRE-AgNPs gradually decreased in accordance with the concentration.

The LC₅₀ and LC₉₀ values for the fourth-instar larvae of *A. aegypti* against the CRE-AgNPs are presented in Table 1. The LC₅₀ and LC₉₀ values of CRE-AgNPs were observed to be 8.963 and 20.515 ppm. The CRE-AgNPs exhibit high toxicity toward the fourth-instar larvae of *A. aegypti* larvae. The CRE showed minimal activity compared to CRE-AgNPs.

The antibacterial activity of the CRE-AgNPs was studied against human pathogenic bacteria such as (a) *S. typhimurium*, (b) *B. subtilis*, (c) *E. faecalis*, and (d) *S. boydii*. CRE-AgNPs had considerable antibacterial activity against the test pathogens, as shown in Figure 7. The CRE-AgNPs in wells showed maximal inhibition compared to the control antibiotic Streptomycin. The maximum antibacterial effect of AgNPs was confirmed by the higher ZOI of CRE-AgNPs compared to that of the control (Table 2). The maximal antimicrobial effect is seen in Ag due to its superficial contact, which inhibits the enzymatic respiratory chain and it also reduces the replication of DNA.

The smaller AgNPs exhibit higher toxicity, which might be due to the larger surface area and fast release of silver ions.^{23,41,42} The zone of inhibition (ZOI) was observed by the well diffusion method, as shown in Table 2.

The cell viability of the CRE-AgNPs was assessed against the HaCaT cell lines (immortalized human keratinocyte cell lines). The cytotoxic effect of HaCaT cells was determined using CRE-AgNPs at various concentrations (5–250 µg/mL). The cytotoxicity of the CRE-AgNPs against HaCaT cells was detected by the MTT assay (shown in Figure 8). The MTT assay was done by cleavage of mitochondrial dehydrogenase in the viable cells by yielding a measurable purple product, which is formazan. The intensity of the dye was measured at 570 nm. The dye concentration is directly proportional to the viable cells and inversely proportional to the toxicity of the cells.⁴³

It should be noted that the CRE-AgNPs have a less cytotoxic effect because 82% of viable cells survive at the concentration of 250 µg/mL. But a lower concentration of CRE-AgNPs shows a vivid cytic effect for the bacteria despite it being less harmful to the HaCaT cells. Earlier, it was stated that the

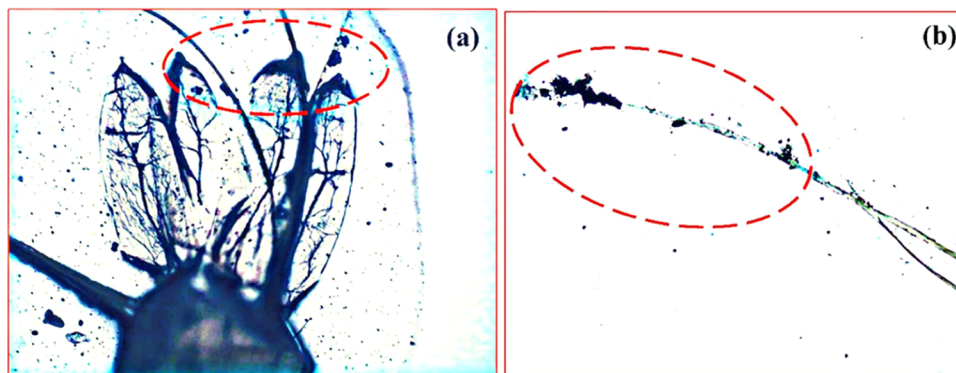


Figure 9. Optical images of *A. Aegypti* larvae treated with CRE-AgNPs (a) show the accumulation of the nanoparticles on the surface of the dorsal plate and anal gills of the larvae and (b) accumulation of the nanoparticles on the siphon hair.

chemically synthesized AgNPs have shown a 30 % cell viability toward the epithelium cell lines.⁴⁴ In this study, CRE-AgNPs show that 82 % of HaCaT cell lines are viable even at a higher concentration.

We found that the CRE-AgNPs accumulated on the lateral hairs of the mosquito larvae. Figure 9 shows the optical image of CRE-AgNPs surrounding the surface of the dorsal plate and anal gills of the larvae, which are absorbed on the posterior part of the larvae. The accumulation of the CRE-AgNPs on the *Aedes Aegypti* larvae may cause morphological damage and restriction in the movement of the larvae. Figure 9b shows nanoparticles attached on the tip of the siphon hair, which may result in the breathing impairment of the larvae.

4. CONCLUSIONS

The structural and larvicidal activity of the CRE-AgNPs was assessed. A simple, economical, efficient, and eco-friendly protocol was employed for the synthesis of AgNPs. Indeed, it is suggested that the CRE-AgNPs were smaller in size, around 30 nm, and highly crystalline in nature. The presence of phytochemicals in plants served as a reducing and capping agent for the CRE-AgNPs. In this work, it was evident that the CRE-AgNPs show 100% mortality and toxicity against the fourth-instar larvae of *A. aegypti*. The lethal concentrations of LC₅₀ and LC₉₀ were observed to be 8.963 and 20.515, respectively, for CRE-AgNPs. CRE-AgNPs are found to be a potentially good candidate for antimicrobial agent against pathogenic bacteria. A lower toxicity of CRE-AgNPs was observed against HaCaT cell lines. Thus, CRE-AgNPs will be considered to be a potential candidate for vector control programs in future.

AUTHOR INFORMATION

Corresponding Authors

Senthil Bakhavatchalam – Department of Chemistry, Faculty of Engineering and Technology, SRM Institute of Science and Technology, Ramapuram Campus, Chennai 600089, India; Phone: +91 9940659448; Email: sen21vino@gmail.com

Junghwan Kim – Department of Materials System Engineering, Pukyong National University, Busan 48513, Republic of Korea; orcid.org/0000-0003-3017-5330; Phone: +82-51-629-6372; Email: junghwan.kim@pknu.ac.kr

Authors

Shanmugam Mahalingam – Department of Materials System Engineering, Pukyong National University, Busan 48513, Republic of Korea

Praveen Kumar Govindaraji – Department of Chemistry, Faculty of Engineering and Technology, SRM Institute of Science and Technology, Ramapuram Campus, Chennai 600089, India

Vasthi Gnanarani Solomon – Department of Chemistry, Faculty of Engineering and Technology, SRM Institute of Science and Technology, Ramapuram Campus, Chennai 600089, India

Hema Kesavan – Department of Chemistry, Faculty of Engineering and Technology, SRM Institute of Science and Technology, Ramapuram Campus, Chennai 600089, India

Yalini Devi Neelan – Department of Materials Science and Engineering, Chungnam National University, Daejeon 34134, Republic of Korea

Prakash Bakhavatchalam – Kings Institute of Preventive Medicine and Research, Chennai 600032, India

Complete contact information is available at:

<https://pubs.acs.org/10.1021/acsomega.2c07531>

Author Contributions

[†]S.M. and P.K.G. contributed equally to this work.

Notes

The authors declare no competing financial interest.

ACKNOWLEDGMENTS

This work was supported by the National Research Foundation of Korea (NRF), grant funded by the Korean government (MSIT) (No. 17111162458). This research was also supported by Basic Science Research Program through the National Research Foundation of Korea (NRF), funded by the Ministry of Education (1345353893).

REFERENCES

- (1) Bhuyar, P.; Rahim, M. H. A.; Sundararaju, S.; Ramaraj, R.; Maniyam, G. P.; Govindan, N. Synthesis of silver nanoparticles using marine macroalgae *Padina* sp. and its antibacterial activity towards pathogenic bacteria. *Beni-Suef Univ. J. Basic Appl. Sci.* **2020**, *9*, No. 3.
- (2) Elumalai, D.; Hemavathi, M.; Rekha, G. S.; Pushpalatha, M.; Leelavathy, R.; Vignesh, A.; Ashok, K.; Babu, M. Photochemical syntheses of silver nanoparticles using *Oscillatoria sancta* micro algae against mosquito vectors *Aedes aegypti* and *Anopheles stephensi*. *Sens. Biosens. Res.* **2021**, *34*, No. 100457.
- (3) Yang, Y. C.; Lee, S. G.; Lee, H. K.; Kim, M. K.; Lee, S. H.; Lee, H. S. A piperidine amide extracted from *Piper longum* L. fruit shows activity against *Aedes aegypti* mosquito larvae. *J. Agric. Food Chem.* **2002**, *50*, 3765–3767.
- (4) Ferdousi, F.; Yoshimatsu, S.; Ma, E.; Sohel, N.; Wagatsuma, Y. Identification of Essential Containers for *Aedes* Larval Breeding to Control Dengue in Dhaka, Bangladesh. *Trop. Med. Health* **2015**, *43*, 253–264.
- (5) Gubler, D. J. The changing epidemiology of yellow fever and dengue, 1900 to 2003: full circle? *Comp. Immunol., Microbiol. Infect. Dis.* **2004**, *27*, 319–330.
- (6) Karthiga, P.; Rajeshkumar, S.; Annadurai, G. Mechanism of Larvicidal Activity of Antimicrobial Silver Nanoparticles Synthesized Using *Garcinia mangostana* Bark Extract. *J. Cluster Sci.* **2018**, *29*, 1233–1241.
- (7) Oves, M.; Rauf, M. A.; Aslam, M.; Qari, H. A.; Sonbol, H.; Ahmad, I.; Zaman, G. S.; Saeed, M. Green synthesis of silver nanoparticles by *Conocarpus Lancifolius* plant extract and their antimicrobial and anticancer activities. *Saudi J. Biol. Sci.* **2022**, *29*, 460–471.
- (8) Oves, M.; Rauf, M. A.; Hussain, A.; Qari, H. A.; Khan, A. A. P.; Muhammad, P.; Rehman, M. T.; Alajmi, M. F.; Ismail, I. I. M. Antibacterial Silver Nanomaterial Synthesis From *Mesoflavibacter zeaxanthinifaciens* and Targeting Biofilm Formation. *Front. Pharmacol.* **2019**, *10*, No. 801.
- (9) Oves, M.; Aslam, M.; Rauf, M. A.; Qayyum, S.; Qari, H. A.; Khan, M. S.; Alam, M. Z.; Tabrez, S.; Pugazhendhi, A.; Ismail, I. M. I. Antimicrobial and anticancer activities of silver nanoparticles synthesized from the root hair extract of *Phoenix dactylifera*. *Mater. Sci. Eng., C* **2018**, *89*, 429–443.
- (10) Velayutham, K.; Rahuman, A. A.; Rajakumar, G.; Roopan, S. M.; Elango, G.; Kamaraj, C.; Marimuthu, S.; Santhoshkumar, T.; Iyappan, M.; Siva, C. Larvicidal activity of green synthesized silver nanoparticles using bark aqueous extract of *Ficus racemosa* against *Culex quinquefasciatus* and *Culex gelidus*. *Asian Pac. J. Trop. Med.* **2013**, *6*, 95–101.

- (11) Dubey, S. P.; Lahtinen, M.; Sillanpaa, M. Tansy fruit mediated greener synthesis of silver and gold nanoparticles. *Process Biochem.* **2010**, *45*, 1065–1071.
- (12) Tran, Q. H.; Nguyen, V. Q.; Le, A.-T. Silver Nanoparticles: Synthesis, Properties, Toxicology, Applications and Perspectives. *Advances in Natural Sciences: Nanoscience and Nanotechnology. Adv. Nat. Sci.: Nanosci. Nanotechnol.* **2013**, *4*, No. 033001.
- (13) Parlinska-Wojtan, M.; Kus-Liskiewicz, M.; Depciuch, J.; Sadik, O. Green synthesis and antibacterial effects of aqueous colloidal solutions of silver nanoparticles using camomile terpenoids as a combined reducing and capping agent. *Bioprocess Biosyst. Eng.* **2016**, *39*, 1213–1223.
- (14) Abdelmoteleb, A.; Gonzalez-Mendoza, D.; Valdez-Salas, B.; Grimaldo-Juarez, O.; Cecaña-Duran, C. Inhibition of *Fusarium solani* in transgenic insect-resistant cotton plants treated with silver nanoparticles from *Prosopis glandulosa* and *Pluchea sericea*. *Egypt. J. Biol. Pest Control* **2018**, *28*, No. 4.
- (15) Das, S.; Sharangi, A. B. Madagascar periwinkle (*Catharanthus roseus* L.): Diverse medicinal and therapeutic benefits to humankind. *J. Pharmacogn. Phytochem.* **2017**, *6*, 1695–1701.
- (16) Nayak, B. S.; Pereira, L. M. P. *Catharanthus roseus* flower extract has wound-healing activity in Sprague Dawley rats. *BMC Complementary Altern. Med.* **2006**, *6*, No. 41.
- (17) Premanath, R.; Sudisha, J.; Devi, N. L.; Aradhya, S. M. Antibacterial and Anti-oxidant Activities of Fenugreek (*Trigonella foenum graecum* L.) Leaves. *Res. J. Med. Plant* **2011**, *5*, 695–705.
- (18) Patil, C. D.; Patil, S. V.; Borase, H. P.; Salunke, B. K.; Salunke, R. B. Larvicidal activity of silver nanoparticles synthesized using *Plumeria rubra* plant latex against *Aedes aegypti* and *Anopheles stephensi*. *Parasitol. Res.* **2012**, *110*, 1815–1822.
- (19) Patil, C. D.; Patil, S. V.; Salunke, B. K.; Salunke, R. B. Larvicidal potential of silver nanoparticles synthesized using fungus *Cochliobolus lunatus* against *Aedes aegypti* (Linnaeus, 1762) and *Anopheles stephensi* Liston (Diptera; Culicidae). *Parasitol. Res.* **2011**, *109*, 823–831.
- (20) WHO. *Report of the WHO Informal Consultation on the Evaluation and Testing of Insecticides*; World Health Organization: Geneva, 1996.
- (21) Rahuman, A. A.; Gopalakrishnan, G.; Ghouse, B. S.; Arumugam, S.; Himalayan, B. Effect of *Feronia limonia* on mosquito larvae. *Fitoterapia* **2000**, *71*, 553–555.
- (22) Bauer, A. W.; Kirby, W. M. M.; Sherris, J. C.; Turck, M. Antibiotic susceptibility testing by a standardized single disk method. *Am. J. Clin. Pathol.* **1966**, *45*, 493–496.
- (23) Yuvarajan, R.; Natarajan, D.; Jayavel, R. Green synthesized silver nanoparticles from *Indoneesiella echioides* and its antibacterial potential. *Indo Am. J. Pharm. Res.* **2014**, *4*, 5121–5128.
- (24) Davoodbasha, M.; Lee, S.-Y.; Kim, S.-C.; Kim, J.-W. One-step synthesis and characterization of broad spectrum antimicrobial efficacy of cellulose/silver nanobiocomposites using solution plasma process. *RSC Adv.* **2015**, *5*, 35052–35060.
- (25) Hussain, S.; Al-Thabaiti, S. A.; Khan, Z. Surfactant-assisted bio-conjugated synthesis of silver nanoparticles (AgNPs). *Bioprocess Biosyst. Eng.* **2014**, *37*, 1727–1735.
- (26) Manjamadha, V. P.; Muthukumar, K. Ultrasound assisted green synthesis of silver nanoparticles using weed plant. *Bioprocess Biosyst. Eng.* **2016**, *39*, 401–411.
- (27) Macdonald, I. D. G.; Smith, W. E. Orientation of cytochrome c adsorbed on a citrate-reduced silver colloid surface. *Langmuir* **1996**, *12*, 706–713.
- (28) Fayaz, A. M.; Balaji, K.; Girilal, M.; Yadav, R.; Kalaichelvan, P. T.; Venketesan, R. Biogenic synthesis of silver nanoparticles and their synergistic effect with antibiotics: a study against gram-positive and gram-negative bacteria. *Nanomed. Nanotechnol. Biol. Med.* **2010**, *6*, 103–109.
- (29) AbdelHamid, A. A.; Al-Ghobashy, M. A.; Fawzy, M.; Mohamed, M. B.; Abdel-Mottaleb, M. M. S. A. Phytosynthesis of Au, Ag, and Au–Ag bimetallic nanoparticles using aqueous extract of sago pondweed (*Potamogeton pectinatus* L.). *ACS Sustainable Chem. Eng.* **2013**, *12*, 1520–1529.
- (30) Kulkarni, A. A.; Bhanage, B. M. Ag@ AgCl nanomaterial synthesis using sugar cane juice and its application in degradation of azo dyes. *ACS Sustainable Chem. Eng.* **2014**, *2*, 007–1013.
- (31) Nhung, T. T.; Lee, S. W. Green synthesis of asymmetrically textured silver meso-flowers (AgMFs) as highly sensitive SERS substrates. *ACS Appl. Mater. Interfaces* **2014**, *6*, 21335–21345.
- (32) Kaszuba, M.; McKnight, D.; Connah, M. T.; McNeil-Watson, F. K.; Nobbmann, U. Measuring sub nanometre sizes using dynamic light scattering. *J. Nanopart. Res.* **2008**, *10*, 823–829.
- (33) Rajasekar, A.; Devasena, T. Facile synthesis of curcumin nanocrystals and validation of its antioxidant activity against circulatory toxicity in Wistar rats. *J. Nanosci. Nanotechnol.* **2015**, *15*, 4119–4125.
- (34) Nadagouda, M. N.; Iyanna, N.; Lalley, J.; Han, C.; Dionysiou, D. D.; Varma, R. S. Synthesis of silver and gold nanoparticles using antioxidants from blackberry, blueberry, pomegranate, and turmeric extracts. *ACS Sustainable Chem. Eng.* **2014**, *2*, 1717–1723.
- (35) Dimitrijevic, R.; Cvetkovic, O.; Miodragovic, Z.; Simic, M.; Manojlovic, D.; Jovic, V. SEM/EDX and XRD characterization of silver nanocrystalline thin film prepared from organometallic solution precursor. *J. Min. Metall., Sect. B* **2013**, *49*, 91–95.
- (36) Gnanadesigan, M.; Anand, M.; Ravikumar, S.; Maruthupandy, M.; Vijayakumar, V.; Selvam, S.; Dhineshkumar, M.; Kumaraguru, A. K. Biosynthesis of silver nanoparticles by using mangrove plant extract and their potential mosquito larvicidal property. *Asian Pac. J. Trop. Med.* **2011**, *4*, 799–803.
- (37) Rajakumar, G.; Rahuman, A. A. Larvicidal activity of synthesized silver nanoparticles using Ecliptaprostrata leaf extract against filariasis and malaria vectors. *Acta Trop.* **2011**, *118*, 196–203.
- (38) Mouchet, F.; Landois, P.; Sarremejean, E.; Bernard, G.; Puech, P.; Pinelli, E.; Flahaut, E.; Gauthier, L. Characterisation and in vivo ecotoxicity evaluation of double-wall carbon nanotubes in larvae of the amphibian *Xenopus laevis*. *Aquat. Toxicol.* **2008**, *87*, 127–137.
- (39) Jayaseelan, C.; Rahuman, A. A.; Rajakumar, G.; Santhoshkumar, T.; Kirthi, A. V.; Marimuthu, S.; Bagavan, A.; Kamaraj, C.; Zahir, A. A.; Elango, G.; Velayutham, K.; Rao, K. V. B.; Karthik, L.; Raveendran, S. Efficacy of plant mediated synthesized silver nanoparticles against hematophagous parasites. *Parasitol. Res.* **2012**, *111*, 921–933.
- (40) Santhoshkumar, T.; Rahuman, A. A.; Rajakumar, G.; Marimuthu, S.; Bagavan, A.; Jayaseelan, C.; Zahir, A. A.; Elango, G.; Kamaraj, C. Synthesis of silver nanoparticles using *Nelumbo nucifera* leaf extract and its larvicidal activity against malaria and filariasis vectors. *Parasitol. Res.* **2011**, *108*, 693–702.
- (41) Xiu, Z. M.; Zhang, Q. B.; Puppala, H. L.; Colvin, V. L.; Alvarez, P. J. J. Negligible particle-specific antibacterial activity of silver nanoparticles. *Nano Lett.* **2012**, *12*, 4271–4275.
- (42) Rai, M.; Yadav, A.; Gade, A. Silver nanoparticles as a new generation of antimicrobials. *Biotechnol. Adv.* **2009**, *27*, 76–83.
- (43) Gurunathan, S. Rapid biological synthesis of silver nanoparticles and their enhanced antibacterial effects against *Escherichia fergusonii* and *Streptococcus mutans*. *Arabian J. Chem.* **2019**, *12*, 168–180.
- (44) Mohanty, S.; Mishra, S.; Jena, P.; Jacob, B.; Sarkar, B.; Sonawane, A. An investigation on the antibacterial, cytotoxic, and antibiofilm efficacy of starch-stabilized silver nanoparticles. *Nanomed.: Nanotechnol. Biol. Med.* **2012**, *8*, 916–924.